Wavefield extrapolation in caustic-free normal ray coordinates

Xuxin Ma and Tariq Alkhalifah, King Abdullah University of Science and Technology

SUMMARY

Normal ray coordinates are conventionally constructed from ray tracing, which inherently requires smooth velocity profiles. To use rays as coordinates, the velocities have to be smoothed further to avoid caustics, which is detrimental to the mapping process. Solving the eikonal equation numerically for a line source at the surface provides a platform to map normal rays in complex unsmoothed velocity models and avoid caustics. We implement reverse-time migration (RTM) and downward continuation in the new ray coordinate system, which allows us to obtain efficient images and avoid some of the dip limitations of downward continuation.

INTRODUCTION

Reverse-time migration (Whitmore, 1983) and downward continuation (Claerbout, 1985) are two commonly used tools for prestack depth imaging in complex geology. Conventionally, the two-way and one-way wave equations are solved on regularly sampled cartesian grids. Cartesian coordinates are favored because its straightforward discretization. However, its usefulness is limited because the wavefront rarely follows x, y or z axis. A coordinate system that follows rays and wavefronts has the benefit that wavefronts have nearly zero curvature.

Alternative coordinate frames have been proposed, for example semi-orthogonal Riemannian coordinates (Sava and Fomel, 2005), which is able to follow rays with overturning angles. However, in complex geology, this method requires excessive smoothing of the velocity model to avoid zero-division at ray caustics. Nonorthogonal Riemannian coordinates (Shragge, 2008) does not require much smoothing, but the complexity of differential operators in nonorthogonal coordinate systems increases the cost for solving the wave equation. Another approach based on vertical time instead of traveltime is free from caustics, however, the coordinates do not follow wavefronts in strong lateral velocity variation (Alkhalifah et al., 2001).

In this abstract, we suggest normal ray mapping that is unconditionally stable in complex media as it uses direct eikonal solvers to develop ray directions. This new coordinate system, which is an orthogonal curvilinear coordinate system, allows us to efficiently and accurately apply downward continuation and RTM. We show impulse responoses to point and line sources that demonstrate the potential of the approach.

THEORY

Normal ray coordinates

The position of a point in space may be determined by its cartesian coordinates $\mathbf{x}$ or any other curvilinear coordinates $\mathbf{u}$, for example $\mathbf{u} = [\rho\ \theta\ \phi]^T$ for spherical coordinates. For a fan of rays u_1 and u_2 are the take-off angle, u_3 could be the traveltime or arclength. For normal rays u_1 and u_2 are the x and y coordinates of shotpoint on the surface. In isotropic media, the ray coordinates system is orthogonal because ray trajectories are always normal to the wavefronts.

Conventionally, ray coordinates are formed by solving the kinematic ray tracing system

$$\begin{aligned} \frac{\mathrm{d}\mathbf{x}}{\mathrm{d}\tau} &= v^2\mathbf{p}, \\ \frac{\mathrm{d}\mathbf{p}}{\mathrm{d}\tau} &= -\frac{\nabla v}{v}, \end{aligned} \tag{1}$$

where $\mathbf{x}$ is a vector defining the location of a point on the wavefront, τ is the traveltime and $\mathbf{p} = \nabla\tau$ is slowness vector, defining the direction of the ray.

One common issue faced by ray coordinates transformation is the mapping of triplications in the traveltime field that occurs in the presence of a strong velocity anomaly. This poses a difficulty when interpolating a function from ray coordinates $\tilde{f}(\mathbf{u})$ to the cartesian coordinates $f(\mathbf{x})$, because of multivalued $\mathbf{u}(\mathbf{x})$.

To avoid such caustics, we are reminded that the solution to the eikonal equation has only the first arrival time. To utilize this feature, rather than computing the slowness vector $\mathbf{p}$ from the second equation in (1), we can use $\mathbf{p}$ calculated from directly solving the eikonal. Thus, instead of (1), ray coordinates can be formed by solving the following system:

$$\begin{aligned} \frac{\mathrm{d}\mathbf{x}}{\mathrm{d}\tau} &= v^2\mathbf{p}, \\ \mathbf{x}(\tau = 0) &= \mathbf{x}_0 \end{aligned} \tag{2}$$

where $\mathbf{x}_0$ is the location of initial wavefront, for a fan of rays it can be a small circle around the shot point, for normal rays it is the surface $z = 0$.

In summary, the complete procedure to construct ray coordinates is

1. solve eikonal for first arrival traveltimes $\tau(\mathbf{x})$
2. compute slowness vector $\mathbf{p}(\mathbf{x}) = \nabla\tau(\mathbf{x})$
3. solve ray tracing system (2) for $\mathbf{x}(\mathbf{u})$

A cartesian space function $f(\mathbf{x})$ can then be interpolated to ray coordinates by simple substitution $\tilde{f}(\mathbf{u}) = f(\mathbf{x}(\mathbf{u}))$.

In order to interpolate from the ray coordinates to the cartesian coordinates, the inverse function to $\mathbf{x}(\mathbf{u})$, i.e. $\mathbf{u}(\mathbf{x})$ needs to be evalutated at every grid. This can be achieved by tracing rays backward starting from every location $\mathbf{x}$ in the space, with the sign of $\mathbf{p}$ reversed in system (2) and terminate ray tracing when $\mathbf{x}$ reaches the surface $z = 0$. The interpolation from ray coordinates to cartesian coordinates is done by substitution $f(\mathbf{x}) = \tilde{f}(\mathbf{u}(\mathbf{x}))$.

DOI http://dx.doi.org/10.1190/segam2012-0104.1

Application to the acoustic wave equation

The acoustic wave equation, casted as a set of first order linear partial differential equations, is given by

$$\rho\frac{\partial w_i}{\partial t} = -\frac{\partial p}{\partial x_i} \quad (i=1,2,3),$$
$$\frac{\partial p}{\partial t} = -k\sum_{i=1}^{3}\frac{\partial w_i}{\partial x_i}, \tag{3}$$

where p is the stress and $\mathbf{w}$ is the particle velocity, ρ is the mass density and k is the bulk modulus.

In an orthogonal curvilinear coordinate system $\mathbf{u}$, the gradient and divergence operators are (Riley et al., 2006)

$$\frac{\partial \phi}{\partial x_i} = \frac{1}{h_i}\frac{\partial \phi}{\partial u_i} \quad (i=1,2,3),$$
$$\sum_{i=1}^{3}\frac{\partial \phi_i}{\partial x_i} = \frac{1}{\prod_{i=1}^{3} h_i}\sum_{i=1}^{3}\frac{\partial}{\partial u_i}\left(\prod_{j\neq i} h_j\phi_i\right), \tag{4}$$

where $h_i = |\partial\mathbf{x}/\partial u_i|$ is a scale factor such that $\mathbf{e}_i = h_i^{-1}\partial\mathbf{x}/\partial u_i$ is a unit vector everywhere tangential to coordinate u_i.

Substituting Equations (4) into Equation (3) yields the ray-coordinate acoustic wave equation

$$\rho\frac{\partial w_i}{\partial t} = -\frac{1}{h_i}\frac{\partial p}{\partial u_i} \quad (i=1,2,3),$$
$$\frac{\partial p}{\partial t} = -\frac{k}{\prod_{i=1}^{3} h_i}\sum_{i=1}^{3}\frac{\partial}{\partial u_i}\left(\prod_{j\neq i}^{3} h_j w_i\right). \tag{5}$$

The second-order scalar wave equation is often used for imaging purposes

$$\frac{1}{v^2}\frac{\partial^2 p}{\partial t^2} = \sum_{i=1}^{3}\frac{\partial^2 p}{\partial x_i^2}, \tag{6}$$

where $v = \sqrt{k/\rho}$ is P-wave velocity.

By combining the two equations in (4), the Laplacian operator in the orthogonal curvilinear coordinate $\mathbf{u}$ is

$$\sum_{i=1}^{3}\frac{\partial^2 \phi}{\partial x_i^2} = \frac{1}{\prod_{i=1}^{3} h_i}\sum_{i=1}^{3}\frac{\partial}{\partial u_i}\left(\frac{\prod_{j\neq i} h_j}{h_i}\frac{\partial \phi}{\partial u_i}\right)$$
$$\approx \sum_{i=1}^{3}\frac{1}{h_i^2}\frac{\partial^2 \phi}{\partial u_i^2}. \tag{7}$$

The approximation in the second line is justified by the fact that odd-order terms in a second-order evolution PDE are diffusive rather than dispersive (Courant and Hilbert, 1989). Thus by dropping the first order terms in this equation the solution retains kinematically correct. Substitute (7) into Equation (6) gives the ray-coordinate two-way wave equation.

$$\frac{1}{v^2}\frac{\partial^2 p}{\partial t^2} = \sum_{i=1}^{3}\frac{1}{h_i^2}\frac{\partial^2 p}{\partial u_i^2}. \tag{8}$$

In the special case when velocity is homogeneous, the normal ray coordinate $\mathbf{u}$ becomes cartesian coordinate $\mathbf{x}$, $h_i = |\partial\mathbf{x}/\partial x_i| = 1$ $(i=1,2,3)$, it is easy to verify that equation (8) reduces to Equation (6).

For example, in two-dimensional space, rays initiated from a line source may be specified by its components shotpoint $u_1 = s$ and traveltime $u_3 = \tau$, in which the scale factors are computed using

$$h_s = \left|\frac{\partial\mathbf{x}}{\partial s}\right| = \sqrt{\left(\frac{\partial x}{\partial s}\right)^2 + \left(\frac{\partial z}{\partial s}\right)^2},$$
$$h_\tau = \left|\frac{\partial\mathbf{x}}{\partial \tau}\right| = \sqrt{\left(\frac{\partial x}{\partial \tau}\right)^2 + \left(\frac{\partial z}{\partial \tau}\right)^2}, \tag{9}$$

for the corresponding wave equation:

$$\frac{1}{v^2}\frac{\partial^2 p}{\partial t^2} = \frac{1}{h_s^2}\frac{\partial^2 p}{\partial s^2} + \frac{1}{h_\tau^2}\frac{\partial^2 p}{\partial \tau^2}. \tag{10}$$

Downward continuation equation

The dispersion relation related to equation (8) is obtained by Fourier transforming it in space and time as follows

$$\frac{\omega^2}{v^2} = \sum_{i=1}^{3}\frac{k_i^2}{h_i^2}. \tag{11}$$

For downward continuation, we can extract the vertical wavenumber

$$k_3 = \pm\frac{\omega h_3}{v}\sqrt{1 - \sum_{i=1}^{2}\frac{v^2 k_i^2}{\omega^2 h_i^2}}, \tag{12}$$

with $+$ for upgoing waves and $-$ for downgoing waves. In the two-dimensional space, the $\omega - k$ downward continuation is

$$k_\tau = \pm\frac{\omega h_\tau}{v}\sqrt{1 - \frac{v^2 k_s^2}{\omega^2 h_s^2}}, \tag{13}$$

and $\omega - x$ downward continuation with, for example, a 15° approximation

$$k_\tau = \pm\frac{\omega h_\tau}{v}\left(1 + \frac{v^2}{2\omega^2 h_s^2}\frac{\partial^2}{\partial x^2}\right). \tag{14}$$

When $h_s = h_\tau = 1$ this equation becomes the cartesian domain 15° paraxial wave equation (Claerbout, 1985).

Mixed domain extrapolators may be derived in a similar fashion. For example, the split-step Fourier migration, k_z can be found using a first-order Taylor expansion about reference slowness $s_0 = 1/v_0$, and thus, the reference scale factors h_{s0} and $h_{\tau 0}$

$$k_\tau \approx \pm h_{\tau 0}\sqrt{\omega^2 s_0^2 - \frac{k_s^2}{h_{s0}^2}}$$
$$+ \omega h_{\tau 0}\Delta s + \omega s_0 \Delta h_\tau + \frac{k_s^2 h_{\tau 0}}{\omega s_0 h_{s0}^3}\Delta h_s, \tag{15}$$

which upon setting $h_s = h_\tau = 1$ and $\Delta h_s = \Delta h_\tau = 0$ reduces to the cartesian-coordinate split-step Fourier migration (Stoffa et al., 1990). In Equation (15) the first term is $\omega - k$ domain

phase shift and the other three terms apply $\omega - x$ domain phase shift. The Δh_s term is still has mixed domain dependence. One simplification could be setting $k_s = 0$ and thus ignore this term (Sava and Fomel, 2005). This could however introduce error to the downward continued wavefield when lateral variation of h_s is large.

EXAMPLES

The presence of a negative anomaly in the velocity causes multi-pathing, and thus triplication of rays and wavefronts. An example of such triplication is illustrated in Figure 1(a) and 1(c), which are computed by the kinematic ray tracing system (1). This could pose a potential difficulty for interpolating from ray coordinates $\mathbf{u}$ to cartesian coordinates $\mathbf{x}$, due to multivalued $\mathbf{u}(\mathbf{x})$ at caustics. By computing rays using eikonal-based ray tracing system (2), such triplications are effectively avoided, because eikonal contains only the first arrival. Our approuch guarantees single valued mapping relations $\mathbf{x}(\mathbf{u})$ and $\mathbf{u}(\mathbf{x})$. An example of such first arrival rays are plotted in Figures 1(b) and 1(d), in which ray caustics below 1500m depth are eliminated.

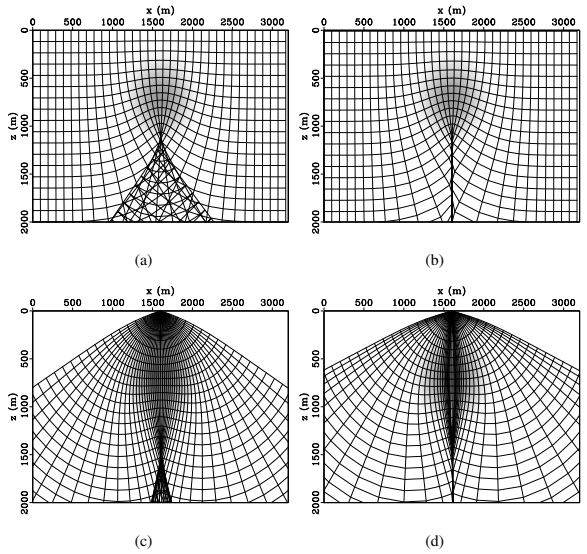

Figure 1: A velocity model overlayed by normal rays (a and b) and a fan of rays (c and d). The velocity includes a -750m/sec anomaly with a homogeneous background of 2250m/sec. Rays in (a) and (c) are computed using Equation (1). Rays in (b) and (d) are computed using Equation (2). Ray caustics below $z = 1500$m are removed in (b) and (d).

As an example of wavefield extrapolation in ray coordinates, we extrapolate a zero-offset section backward in time and in depth, in both cartesian coordinates and normal ray coordinates, and compare the results. The zero-offset data has horizontal events at 0.44sec, 0.84sec and 1.24sec. The velocity model has a background linear gradient and a negative lens anomaly, as shown in Figure 2(a). Figure 2(b) is the same velocity interpolated to normal ray coordinates, which has horizontal axis of shotpoint s and vertical axis of traveltime τ. The wavefield could also be extrapolated in ray coordinates initiated from a point, in which case the horizontal axis is take-off angle.

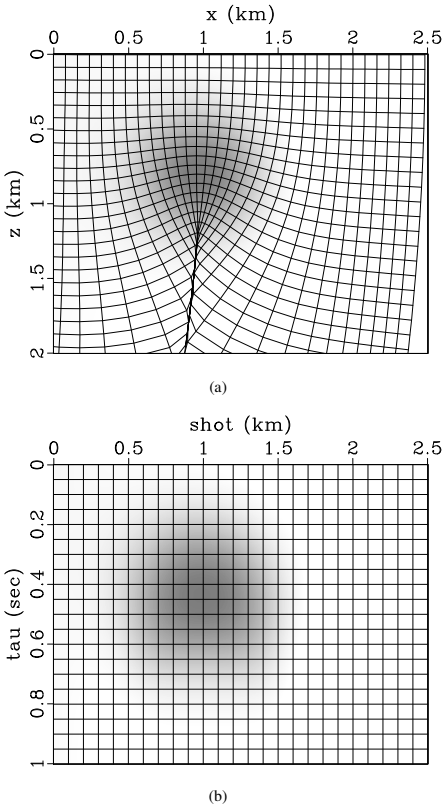

Figure 2: (a) Velocity model overlayed by normal ray coordinates. The background velocity is $2100 + 0.025z + 0.14x$ m/sec and the lens has a -750m/sec velocity perturbation. (b) The velocity interpolated to the normal ray coordinates.

Figure 3(b) is the image obtained from poststack reverse-time migration in the cartesian domain, using the two-way wave equation (6). In the normal ray coordinates, reverse-time migration is achieved by solving Equation (10). This result is plotted in Figure 3(c). As expected, the reflectors in ray coordinates are flat because the surface $\tau = \text{const}$ is always tangential to first arrival wavefronts. To check consistency of migration in the two domains, the image obtained in normal ray coordinates is interpolated to cartesian coordinates, in Figure 3(d). The agreement between Figure 3(b) and 3(d) verifies the correctness of the ray-coordinates two-way wave equation (10).

Similar to the horizontal events, we computed the impulse response of reverse-time migration in cartesian and normal ray coordinates. The migration images are plotted in Figures 4(b) to 4(d). Again, the two migration images are consistent.

Downward continuation in normal ray coordinates is achieved by solving the corresponding one-way wave equation. In this particular example, we use the split-step Fourier migration de-

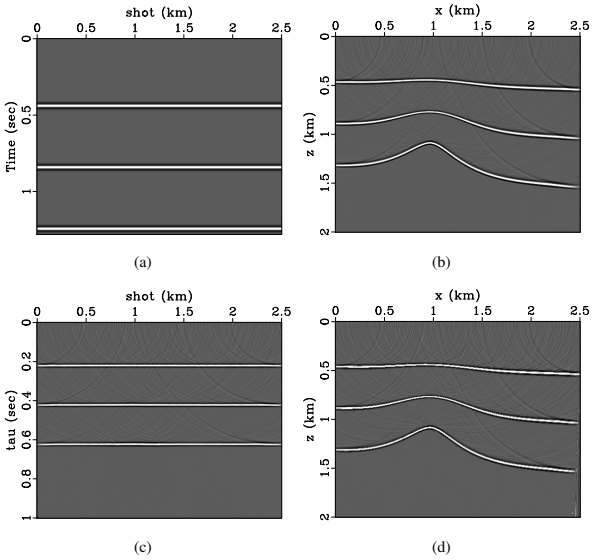

Figure 3: Poststack reverse-time migration. (a) zero-offset data featuring three horizontal events at 0.44sec, 0.84sec and 1.24sec. Migration images obtained in (b) cartesian coordinates and (c) normal ray coordinates. (d) shows the image (b) interpolated to cartesian coordinates.

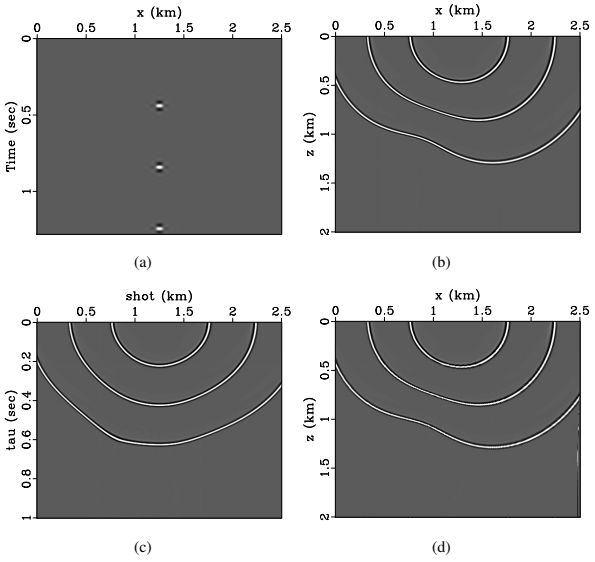

Figure 4: Impulse response of poststack reverse-time migration. (a) zero-offset data featuring three spikes at 0.44sec, 0.84sec and 1.24sec. Migration images obtained in (b) cartesian coordinates and (c) normal ray coordinates. (d) shows the image (b) interpolated to cartesian coordinates.

scribed by Equation (15). The migration images of the same zero-offset data are plotted in Figure 5(a) for cartesian coordinates and in Figure 5(b) for the ray coordinates result interpolated to cartesian coordinates. The impulse responses of these two migration operators are plotted in Figures 6(a) and 6(b).

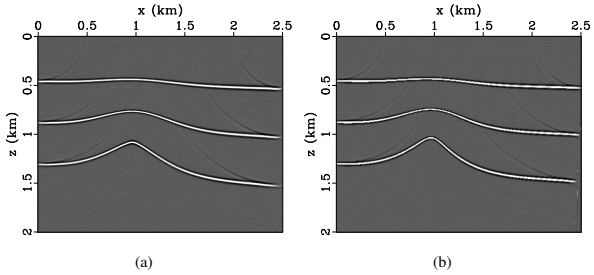

Figure 5: Poststack split-step Fourier migration of data in Figure 3(a), showing (a) cartesian coordinates migration image (b) normal ray coordinates migration image interpolated to cartesian coordinates.

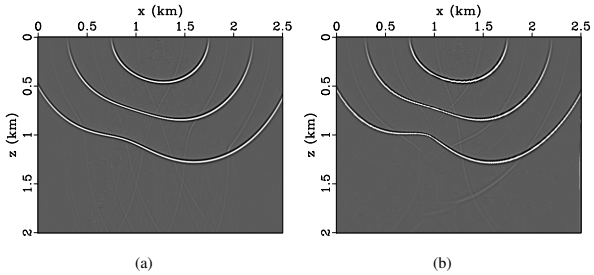

Figure 6: Impulse response of poststack split-step Fourier migration, showing (a) cartesian coordinates migration image (b) normal ray coordinates migration image interpolated to cartesian coordinates.

In both Figures 5(b) and 6(b), the discrepancies observed near $x = 1$km of the deep reflector is an indication of the error due to $k_s = 0$ assumption, as addressed previously with Equation (15).

CONCLUSION

We introduced an approach to construct normal ray coordinates based on first arrival traveltimes. Interpolation between the cartesian coordinates and the ray coordinates are free from caustics. We derived a two-way acoustic equation and one-way downward continuation equations for normal ray coordinates. Using these equation, zero-offset sections are migrated in both cartesian and normal ray coordinates using reverse-time migration and downward continuation. The migration images obtained by reverse-time migration in the cartesian and normal ray coordinates are consistent. Downward continuation in normal ray coordinates less accurate because of ignoring lateral variation of h_s.

ACKNOWLEDGEMENTS

We are grateful to KAUST for supporting this research. We thank Anton Duchkov for helpful discussions.

DOI http://dx.doi.org/10.1190/segam2012-0104.1

http://dx.doi.org/10.1190/segam2012-0104.1

EDITED REFERENCES

Note: This reference list is a copy-edited version of the reference list submitted by the author. Reference lists for the 2012 SEG Technical Program Expanded Abstracts have been copy edited so that references provided with the online metadata for each paper will achieve a high degree of linking to cited sources that appear on the Web.

REFERENCES

Alkhalifah, T., S. Fomel, and B. Biondi, 2001, The space-time domain: theory and modelling for anisotropic media: Geophysical Journal International, **144**, 105-113.

Claerbout, J. F., 1985, Imaging the earth's interior: Blackwell Scientific Publications.

Courant, R., and D. Hilbert, 1989, Methods of mathematical physics: John Wiley & Sons.

Riley, K., M. Hobson, and S. Bence, 2006, Mathematical methods for physics and engineering: Cambridge University Press.

Sava, P., and S. Fomel, 2005, Riemannian wavefield extrapolation: Geophysics, **70**, no. 3, T45-T56.

Shragge, J. C., 2008, Riemannian wavefield extrapolation: Nonorthogonal coordinate systems: Geophysics, **73**, no. 2, T11-T21.

Stoffa, P. L., J. T. Fokkema, R. M. de Luna Freire, and W. P. Kessinger, 1990, Split-step Fourier migration: Geophysics, **55**, 410-421.

Whitmore, N. D., 1983, Iterative depth migration by backward time propagation: SEG Technical Program Expanded Abstracts, **2**, 382-385.